Power Control Optimization for Multibeam Joint Communication and Sensing Systems

Caio G. de Figueredo, Walter C. Freitas Jr, Yuri C. B. Silva, *Member, IEEE*, Roberto P. Antonioli, and Gábor Fodor, *Fellow, IEEE*

***Abstract*—The multibeam technique, which enables antenna arrays to produce several beams or lobes in different directions, has been proposed to enable integrated sensing and communication for the upcoming sixth-generation of mobile communication systems. In this work, while adopting the multibeam technique, we optimize the power distribution between communication and sensing beams. Imposing constraints on the communication to ensure a minimum performance level, we look for the power control coefficient value that optimizes one of three suitable objective functions for sensing: the sensing signal-to-interference-plus-noise ratio, the Cramér-Rao lower bound of the angle-of-arrival estimator, and the mutual information between the sensing channel and the echo signals from the targets. We find that multibeam modeling leads to convex optimization problems, which are therefore suitable for real-time implementation. Our scheme manages the inherent trade-off involved in balancing the power between communication and sensing by using the optimum power coefficient. The numerical results show an improvement of the beam shape and the relevant performance metrics compared with the radiation pattern obtained by previously proposed multibeam schemes.**

***Index Terms*—joint communication and sensing, multibeam antenna array, power allocation, communication and sensing performance metrics.**

I. Introduction

Joint communication and sensing (JCAS) is expected to become one of the technologies, specifically targeting beyond communication services, in the upcoming sixth-generation of mobile communication systems (6G). Together with a cell-free architecture, it is expected to provide high data rate communication, while incorporating environment sensing for many applications such as vehicle tracking, traffic monitoring, weather prediction and sensing-assisted communication [1].

There are many open research trends in this emerging field, which demonstrate how challenging it is for designers to integrate radar and communication services in a single system [2]. Regarding beamforming (BF) techniques [3], the main challenge is that both functionalities have different BF requirements: for communication, it is important to have a fixed narrower beam directed towards the users; while for sensing, it is useful to have a broader varying beam for scanning the environment while detecting and tracking targets.

An important recent development to tackle the aforementioned problem is the multibeam technique, which allows for simultaneous communication and sensing by using a single antenna array with multiple beams or multiple lobes in different directions [4], [5]. Several array configurations for multibeam are developed in recent literature, such as analog steerable arrays [4] and hybrid analog-and-digital structures [6]. Specifically, in [4] – one of the pioneering works in this field – two multibeam methods, using a single radio frequency chain, are developed. In the first one, named M1-Zhang by the authors, the communication and sensing BF vectors are generated separately and combined using a power distribution coefficient and a phase shift term. In the second one, named M2-Zhang, the BF vector is generated in a joint manner. Both of them use an algorithm called iterative least-squares [7] to generate the desired beam shape. Some other papers of the same authors discuss optimum BF design proposing a series of different optimization methods [8]–[10]. More recent works in this field employ multibeam in different optimization problems, for example, in [11], where the BF design relies on the maximization of the peak sidelobe level, i.e., the difference between the desired main lobe and the secondary ones. In [12], where both the BF vectors and waveforms are optimized using the receiver gain and the Cramér-Rao Lower Bound (CRLB) of the target distance estimate. In these latter two papers, the modelling leads to non-convex optimization problems.

Another question that arises is how to properly balance resources, like power, bandwidth and processing time, between communication and sensing. To this end, the first task is to determine a set of metrics to properly quantify the sensing and communication performances. In [13], signal-to-interference-plus-noise ratio (SINR) is used to design a multi-static radar integrated in a cellular network. In [14], probability of detection, CRLB and posterior CRLB are used to quantify the quality-of-service (QoS) for sensing, localization and tracking. In [15], the authors have formulated an optimization problem also based on the SINR for both sensing and communication. In [16]–[18], the CRLB, and in [19], the mutual information (MI) between the echo signals from the targets and the sensing channel are used as metrics for the sensing. More recent works,

Caio G. de Figueredo is with Instituto Federal do Ceará (IFCE), Boa Viagem - CE, Brazil, and Wireless Telecommunications Research Group (GTEL), Federal University of Ceara, Fortaleza - CE, Brazil, e-mail: caio@gtel.ufc.br.

Walter C. Freitas Jr, Yuri C. B. Silva and Roberto Pinto Antonioli are with Wireless Telecommunications Research Group (GTEL), Federal University of Ceara, Fortaleza - CE, Brazil. (e-mail: walter@gtel.ufc.br; yuri@gtel.ufc.br; antonioli@gtel.ufc.br).

Gábor Fodor is with Ericsson Research, 16480 Stockholm, Sweden, and also with the Division of Decision and Control, KTH Royal Institute of Technology, 11428 Stockholm, Sweden, e-mail: gabor.fodor@ericsson.com.

This work was supported in part by Ericsson Research, Technical Cooperation Contracts UFC.50 and UFC.52, in part by the Brazilian National Council for Scientific and Technological Development (CNPq), in part by CAPES - Finance Code 001, in part by FUNCAP under grants ITR-0214-00041.01.00/23 and UNI-0210-00043.01.00/23. G. Fodor was supported by the Swedish Strategic Foundation Future Software Systems Project SAICOM, Grant No: FUS21-0004.

like [20] and [21], had developed a novel information-theoretic metric called capacity-distortion, where this single metric to characterize communication and sensing performances was proposed.

In this paper, we extend the works in [4], [5] by using three of the aforementioned metrics to optimize the power balance between communication and sensing: SINR, CRLB and MI. We consider a bi-static sensing with two access points (AP), where only the transmitter AP communicates with the user equipment (UE) and sends the sensing signal using the multibeam technique, the receiver AP receives the echo signals from the targets. The results show an improvement in the sensing performance in terms of probability of detection and in the beam shape when compared to the methods developed in [4], [8]–[10]. They also show the trade-off between communication and sensing in terms of the aforementioned metrics and spectral efficiency. The main contributions of this paper are:

- We propose three different ways to optimize the power balance between sensing and communication; these results are summarized in Eq. (13), (20) and (27). Unlike [11], [12], we demonstrate that our multibeam modeling for the transmitter BF leads to three convex optimization problems that are well suited for real-time applications due to its simplicity.
- We compare the above three techniques, which helps to gain insight into the values obtained for the power coefficient. We also compare the behavior of the three metrics when using static and optimized values for the power coefficient.

In Tab. I we summarize a brief comparison with related works.

II. System Model

We consider a bi-static scenario with K targets: one transmitter AP with L-element uniform linear array (ULA) for sensing and communication, and one receiver AP with M-element ULA just for sensing. We also consider a downlink communication between the transmitter and a single antenna user. This scenario is depicted in Fig. 1. The received sensing signal in [5] can be rewritten more compactly as [6],

$$\mathbf{y}[m] = \mathbf{H}\mathbf{x}[m] + \mathbf{n}[m] \in \mathbb{C}^{M\times 1}, \tag{1}$$

where

$$\mathbf{x}[m] = \mathbf{w}\cdot p[m] \in \mathbb{C}^{L\times 1} \tag{2}$$

is the transmitted signal, with $\mathbf{w} \in \mathbb{C}^{L\times 1}$ is the precoder and $p[m] \sim \mathcal{CN}(0,1)$ as the symbol to be transmitted at time instant m; also,

$$\mathbf{n}[m] \sim \mathcal{CN}(\mathbf{0}, \sigma_s^2 \mathbf{I}_M) \in \mathbb{C}^{M\times 1} \tag{3}$$

is the sensing noise vector. The sensing channel matrix is

$$\mathbf{H} = \mathbf{A}_M(\Theta)\boldsymbol{\Gamma}\mathbf{A}_L^H(\Phi) \in \mathbb{C}^{M\times L}, \tag{4}$$

whose composing matrices

$$\mathbf{A}_M(\Theta) = \left[\mathbf{a}_M(\theta_1)\cdots\mathbf{a}_M(\theta_K)\right] \in \mathbb{C}^{M\times K}, \tag{5}$$
$$\mathbf{A}_L(\Phi) = \left[\mathbf{a}_L(\phi_1)\cdots\mathbf{a}_L(\phi_K)\right] \in \mathbb{C}^{L\times K} \tag{6}$$

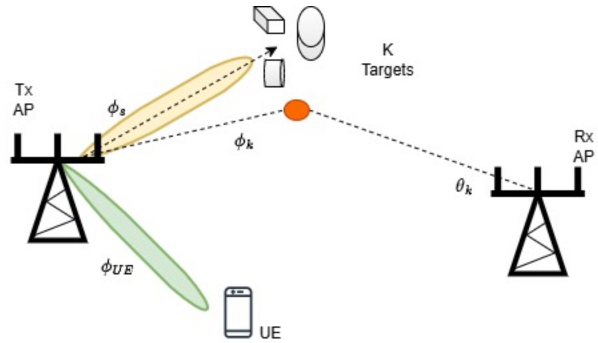

Fig. 1: System model employed in this paper.

collect the array steering vectors, $\mathbf{a}_M$ and $\mathbf{a}_L$, for the receiver and the transmitter; $\Theta = \{\theta_1, \cdots, \theta_K\}$ and $\Phi = \{\phi_1, \cdots, \phi_K\}$, where θ_k and ϕ_k are the angles of arrival (AoA) and the angles of departure (AoD) for the k-th target, respectively; $\boldsymbol{\Gamma} = \operatorname{diag}(\gamma_1, \cdots, \gamma_K)$ is a diagonal matrix whose elements are the reflection coefficients of the K targets, such that for the k-th one we have $\gamma_k \sim \mathcal{CN}(0, \sigma_k^2)$ [15].

The communication signal received at the single antenna UE [5] is

$$y_{\mathrm{UE}}[m] = \mathbf{h}^H \mathbf{x}[m] + z[m] \in \mathbb{C}, \tag{7}$$

where

$$\mathbf{h} = \gamma_{\mathrm{UE}}\mathbf{a}_L(\phi_{\mathrm{UE}}) \in \mathbb{C}^{L\times 1} \tag{8}$$

is the communication channel vector, ϕ_{UE} is the angle of departure for the user equipment, γ_{UE} is the path loss coefficient and $z[m] \sim \mathcal{CN}(0, \sigma_{\mathrm{UE}}^2)$ is the communication noise.

The multibeam precoder is

$$\mathbf{w} = \sqrt{\delta L^{-1}}\mathbf{a}_L(\phi_s) + \sqrt{(1-\delta)L^{-1}}\mathbf{a}_L(\phi_{\mathrm{UE}}) \in \mathbb{C}^{L\times 1}, \tag{9}$$

where we assume that the transmitter knows ϕ_{UE}, which is a reasonable assumption since it can be estimated when receiving the uplink signal from the UE, $\delta \in (0,1)$ is the power control coefficient and ϕ_s is the sensing angle in the direction of the cluster of targets. It is important to emphasize the difference between ϕ_k and ϕ_s: the former is the actual angle of departure for the k-th target, the latter is the central angle of the sensing beam. This difference is illustrated in Fig. 1

III. Power Coefficient Optimization

In this section, we consider optimization strategies for computing the power control coefficient δ, based on three different sensing objective functions: the sensing SINR [22], the CRLB of the AoA estimator and the MI [16], while subject to minimum communication SINR constraint.

A. Signal-to-Interference-Plus-Noise Ratio

For the sake of simplicity, we can rewrite Eq. (9) as

$$\mathbf{w} = \sqrt{\delta}\mathbf{w}_s + \sqrt{1-\delta}\mathbf{w}_{\mathrm{UE}}, \tag{10}$$

TABLE I: Related works comparison

Publication	Multibeam	Multi-static sensing	Power allocation	Obj. func. comparison
[16]	Yes	No	No	Yes
[4]	Yes	No	No	No
[6]	Yes	No	No	No
[12]	Yes	No	No	No
[11]	Yes	No	No	No
[14]	No	No	Yes	Yes
This paper	Yes	Yes	Yes	Yes

where $\mathbf{w}_s = \sqrt{L^{-1}}\mathbf{a}_L(\phi_s)$ and $\mathbf{w}_{\mathrm{UE}} = \sqrt{L^{-1}}\mathbf{a}_L(\phi_{\mathrm{UE}})$. The communication received signal can be written as

$$y_{\mathrm{UE}}[m] = \sqrt{1-\delta}\cdot\mathbf{h}^H\mathbf{w}_{\mathrm{UE}}p[m] + \sqrt{\delta}\cdot\mathbf{h}^H\mathbf{w}_s p[m] + z[m],$$

where the first term on the right side of the equation is the desired communication signal and the second term is the interference from the sensing signal. Hence, the communication SINR is defined as

$$\mathrm{SINR}_{\mathrm{UE}}(\delta) = \frac{(1-\delta)|\mathbf{h}^H\mathbf{w}_{\mathrm{UE}}|^2}{\delta|\mathbf{h}^H\mathbf{w}_s|^2 + \sigma^2_{\mathrm{UE}}}. \tag{11}$$

In a similar manner, the sensing received signal can be written as

$$\mathbf{y}[m] = \sqrt{\delta}\mathbf{H}\mathbf{w}_s p[m] + \sqrt{1-\delta}\mathbf{H}\mathbf{w}_{\mathrm{UE}}p[m] + \mathbf{n}[m],$$

where the first term on the right side of the above equation is the desired sensing signal and the second term is the interference from the communication signal. The sensing SINR is defined as

$$\mathrm{SINR}_s(\delta) = \frac{\delta\|\mathbf{H}\mathbf{w}_s\|^2}{(1-\delta)\|\mathbf{H}\mathbf{w}_{\mathrm{UE}}\|^2 + M\sigma_s^2}. \tag{12}$$

Using Eq. (12) as objective function and Eq. (11) as constraint, the optimization problem is

$$\begin{aligned} \underset{\delta}{\text{maximize}} \quad & \mathrm{SINR}_s(\delta), \\ \text{s.t.} \quad & \mathrm{SINR}_{\mathrm{UE}}(\delta) \geq \lambda, \\ & 0 < \delta < 1. \end{aligned} \tag{13}$$

B. Cramér-Rao Lower Bound

Another metric that can be used to optimizing the power distribution between sensing and communication is the CRLB of one of the estimators employed at the receiver AP. The CRLB of an unbiased vector estimator is a square matrix whose main diagonal elements are the lower limits for the variances of the estimation error. Departing from a well-known CRLB expression, we intend to minimize it under the same constraint on the communication. In this paper we use the CRLB for the AoA estimator, which is defined as [23]

$$\mathbf{CRLB}(\Theta) = \mathbf{F}^{-1} \in \mathbb{R}^{K\times K},$$

where $\mathbf{F}$ is the so-called Fisher information matrix which, for our system model, is given by [24]

$$\mathbf{F} = \frac{2}{\sigma_s^2}\sum_{n=0}^{\lfloor\alpha N\rfloor-1}\mathrm{Re}\left\{\mathbf{S}^H[m]\mathbf{D}^H(\Theta)\mathbf{D}(\Theta)\mathbf{S}[m]\right\}, \tag{14}$$

where N is the number of slots in a frame that corresponds to a coherence block, α is the proportion of this frame in which the sensing beam points to one fixed direction, and

$$\mathbf{D}(\Theta) = \left[\left(\frac{\partial\mathbf{a}_M(\psi)}{\partial\psi}\right)_{\psi=\theta_1} \cdots \left(\frac{\partial\mathbf{a}_M(\psi)}{\partial\psi}\right)_{\psi=\theta_K}\right] \in \mathbb{C}^{M\times K}, \tag{15}$$

$$\mathbf{S}[m] = \mathrm{diag}\left\{\mathbf{\Gamma}\mathbf{A}_L^H\mathbf{w}p[m]\right\} \in \mathbb{C}^{K\times 1}. \tag{16}$$

These expressions for the CRLB are demonstrated in Appendix A. We can minimize the CRLB trace subject to the same constraint imposed in the previous problem, but it is more computationally efficient to avoid the matrix inversion. Let us first develop Eq. (16) using the definition of $\mathbf{w}$ in Eq. (9), in order to see more clearly the dependence on δ. We have

$$\mathbf{S}[m] = \left(\mathbf{S}_{\mathrm{s}}\sqrt{\delta L^{-1}} + \mathbf{S}_{\mathrm{UE}}\sqrt{(1-\delta)L^{-1}}\right)p[m], \tag{17}$$

where $\mathbf{S}_{\mathrm{s}} = \mathrm{diag}\left(\mathbf{\Gamma}\mathbf{A}_L^H\mathbf{a}_L(\phi_s)\right)$ and $\mathbf{S}_{\mathrm{UE}} = \mathrm{diag}\left(\mathbf{\Gamma}\mathbf{A}_L^H\mathbf{a}_L(\phi_{\mathrm{UE}})\right)$. Replacing $\mathbf{S}[m]$ in $\mathbf{F}$, and after some algebraic manipulation, we have

$$\mathbf{F} = \mathbf{A}_1\delta + \mathbf{A}_2\sqrt{\delta(1-\delta)} + \mathbf{A}_3(1-\delta), \tag{18}$$

where $\mathbf{A}_1$, $\mathbf{A}_2$ and $\mathbf{A}_3$ are matrix constants that do not depend on δ. If we take the Frobenius norm of $\mathbf{F}$ and use the triangle inequality, we can write

$$\begin{aligned} \|\mathbf{F}\|_F &= \|\mathbf{A}_1\delta + \mathbf{A}_2\sqrt{\delta(1-\delta)} + \mathbf{A}_3(1-\delta)\|_F \\ &\leq \|\mathbf{A}_1\|_F\delta + \|\mathbf{A}_2\|_F\sqrt{\delta(1-\delta)} + \|\mathbf{A}_3\|_F(1-\delta), \\ &= \|\mathbf{F}\|_F^{max}(\delta). \end{aligned} \tag{19}$$

This last expression gives the maximum value for the Frobenius norm of $\mathbf{F}$. If we maximize this upper limit, we end up maximizing $\|\mathbf{F}\|_F$, which, as a consequence, results in minimizing the norm of the CRLB. Therefore, using Eq. (19) as objective function and the same set of constraints as in Eq. (13), the optimization problem remains

$$\begin{aligned} \underset{\delta}{\text{maximize}} \quad & \|\mathbf{F}\|_F^{max}(\delta) \\ \text{s.t.} \quad & \mathrm{SINR}_{\mathrm{UE}}(\delta) \geq \lambda, \\ & 0 < \delta < 1. \end{aligned} \tag{20}$$

C. Mutual Information

One final alternative for the sensing metric is the mutual information between the sensing channel and the echo sig-

TABLE II: Simulation parameters for Figs. 2 - 3.

Parameters	Value
Number of targets K	5
Number of Tx antennas L	16
Number of Rx antennas M	16
Number of slots in a frame N	160
Sensing noise variance σ_s^2	0 dBW
Communication beam direction ϕ_{UE}	99^o
Sensing beam direction ϕ_s	83^o
Angles of departure for the targets Φ	$\{79^o\, 81^o\, 83^o\, 85^o\, 87^o\}$
Angles of arrival Θ	$\{60^o\, 80^o\, 100^o\, 120^o\, 140^o\}$

nals [16]. If we collect the sensing signal samples in a frame, Eq. (1) can be written as

$$\mathbf{Y} = \mathbf{H}\mathbf{X}(\delta) + \mathbf{N}, \tag{21}$$

where the echo signal and the sensing noise are

$$\mathbf{Y} = [\mathbf{y}[0] \cdots \mathbf{y}[\lfloor \alpha N \rfloor - 1]] \in \mathbb{C}^{M \times \lfloor \alpha N \rfloor}, \tag{22}$$
$$\mathbf{N} = [\,\mathbf{n}[0] \cdots \mathbf{n}[\lfloor \alpha N \rfloor - 1]\,] \in \mathbb{C}^{M \times \lfloor \alpha N \rfloor}, \tag{23}$$

and the transmitted signal is

$$\mathbf{X}(\delta) = \mathbf{w}(\delta) \cdot \mathbf{p}^T = \mathbf{w} \cdot [\,p[0] \;\cdots\; p[\lfloor \alpha N \rfloor - 1]\,] \in \mathbb{C}^{L \times \lfloor \alpha N \rfloor}, \tag{24}$$

where we recall the dependency of $\mathbf{w}$ on δ. The MI between the channel and the received sensing signal is defined as [19]

$$I(\mathbf{H}; \mathbf{Y}|\mathbf{X}) = H(\mathbf{Y}|\mathbf{X}) - H(\mathbf{N}), \tag{25}$$

where $H(\cdot)$ is the differential entropy of a random variable. For our particular model, it can be demonstrated to be given by

$$I(\delta) = M \log_2 \left\{ \det \left[\sigma_s^{-2} \mathbf{X}(\delta)^T \mathbf{\Sigma}_H \mathbf{X}(\delta)^* + \mathbf{I}_{\lfloor \alpha N \rfloor} \right] \right\}, \tag{26}$$

where $\mathbf{\Sigma}_H$ is the spatial correlation matrix of the channel, i.e., $\mathbf{\Sigma}_H = \mathbb{E}\{\mathbf{H}^H \mathbf{H}\}$. We want to maximize MI in order to obtain as much information about the channel from the echo signals as possible. Hence, using $I(\delta)$ as objective function and the same set of constraints of the previous problems, the MI optimization is

$$\begin{aligned} \underset{\delta}{\text{maximize}} \quad & I(\delta) \\ \text{s.t.} \quad & \mathrm{SINR}_{\mathrm{UE}}(\delta) \geq \lambda, \\ & 0 < \delta < 1. \end{aligned} \tag{27}$$

IV. Numerical Results

The simulation parameters considered in this first set of experiments, which comprises Fig. 2 - 3, are: the number of targets to scan is $K = 5$; the sensing noise variance is $\sigma_s^2 = 0\,\mathrm{dBW}$; the sensing angles of departure are spread around $\phi_s = 83^{\mathrm{o}}$, and the communication angle of departure is $\phi_{\mathrm{UE}} = 99^{\mathrm{o}}$; the angles of arrival are $\Theta = \{60^{\mathrm{o}}, 80^{\mathrm{o}}, 100^{\mathrm{o}}, 120^{\mathrm{o}}, 140^{\mathrm{o}}\}$. These parameters are summarized in Tab. II.

In Figs. 2a - 2c, we show how the three objective functions depend on the communication noise variance σ^2_{UE}. We intend to compare their behavior for the optimum value of δ, which changes for each σ^2_{UE}, and for some static values. For static δ, the functions are unchangeable because the same transmitting power on the sensing beam is kept. Hence, we notice that

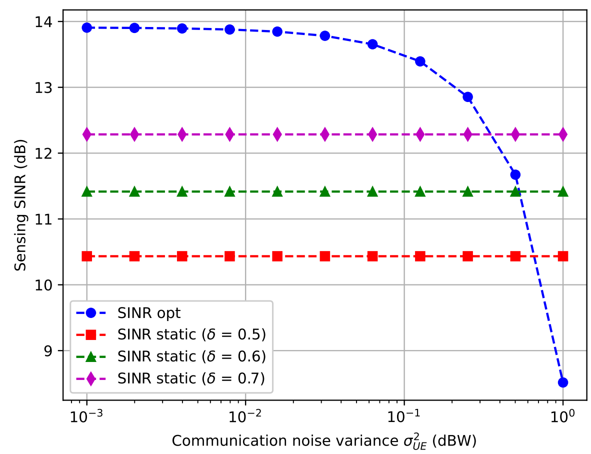

(a)

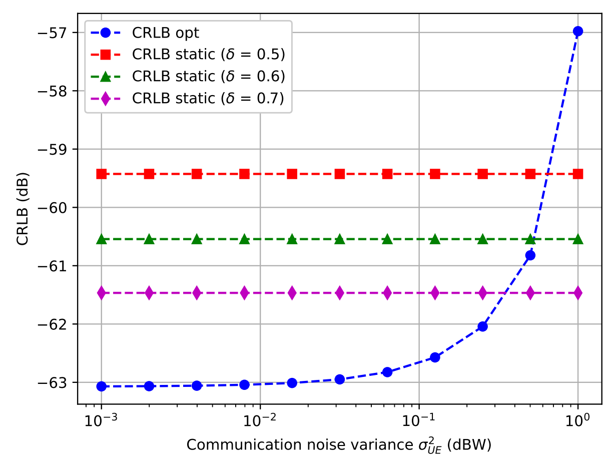

(b)

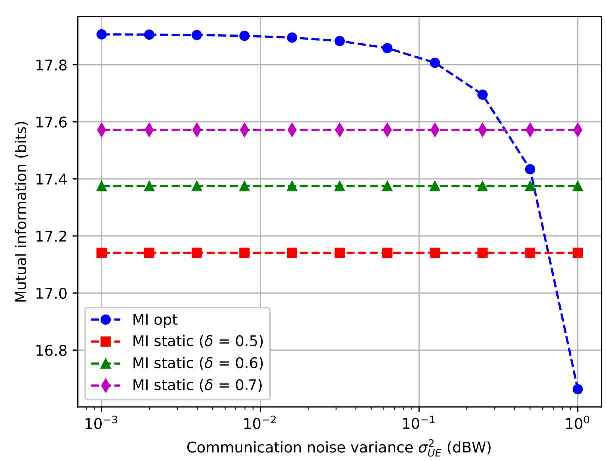

(c)

Fig. 2: (a) Sensing SINR, (b) CRLB and (c) MI versus communication noise variance (σ^2_{UE}).

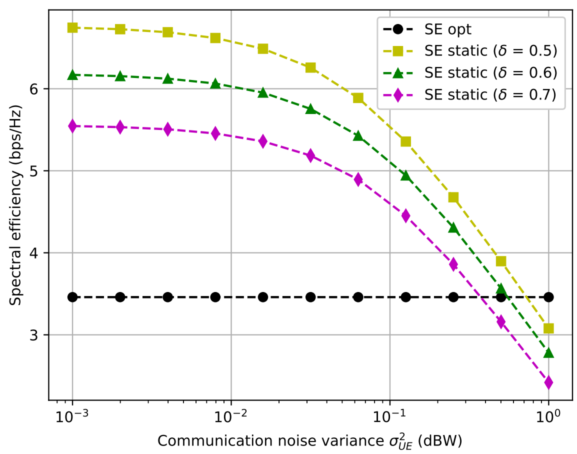

Fig. 3: Spectral efficiency versus communication noise variance (σ^2_{UE}).

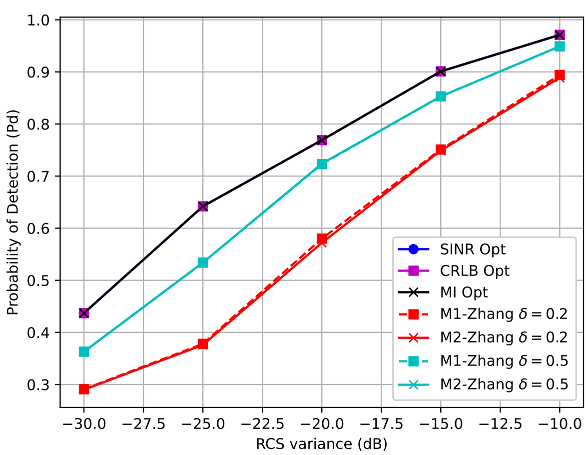

Fig. 4: Probability of detection versus radar cross-section (RCS) variance.

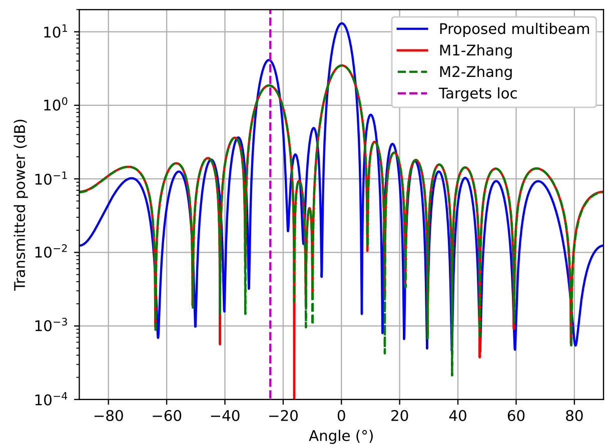

Fig. 5: Radiation pattern of the transmitter antenna.

TABLE III: Simulation parameters for Figs. 4 and 5

Parameters	**Value**
Number of targets K	1
Number of Tx and Rx antennas L	16
Number of Rx antennas M	16
Number of slots in a frame N	160
Communication noise variance σ^2_{UE}	-10 dBW
Sensing noise variance σ^2_s	0 dBW
Communication beam direction ϕ_{UE}	0^o
Sensing beam direction ϕ_s	-24.4^o
Angle of arrival θ	45^o

this static scheme is advantageous only for high levels of communication noise. However, it comes at the expense of communication performance, as we can see in Fig. 3, where the decrease in spectral efficiency is clear as σ^2_{UE} increases. On the other hand, when power optimization is employed, it is possible to manage power towards the communication beam as the communication noise increases, keeping the communication performance at a minimum accepted level, as we also can see in Fig. 3, where the spectral efficiency is kept constant independent of the noise power.

We also performed a second set of experiments with the following simulation parameters: we assume a single target scenario, i.e., the number of targets to scan is $K = 1$; the sensing noise variance is $\sigma^2_s = 0\,\mathrm{dBW}$; the sensing angle of departure is $\phi_s = -24.4^{\mathrm{o}}$, and the communication angle of departure is $\phi_{\mathrm{UE}} = 0^{\mathrm{o}}$; the angle of arrival is $\theta = 45^{\mathrm{o}}$. These parameters are summarized in Tab. III.

In Fig. 4, we show the probability of detection (P_d) of a single target as its RCS variance varies from -30 to -10 dB. We use M1-Zhang and M2-Zhang as benchmarks for comparison. The RCS is a parameter that quantifies how hard is to detect the target: the smaller its variance is, the harder is to detect it. We performed a Monte Carlo simulation, with 1000 iterations, where 160 known symbols are transmitted by one AP and received by the other, in bi-static sensing scenario depicted earlier. When the receiver detects the echo signal, it performs a simple binary hypothesis test to decide about the target's presence. In order to determine the threshold to be employed, we set the probability of false alarm $P_{FA} = 0.1$. In each iteration, we calculate, for the proposed method, the optimum value of the power coefficient δ, whereas for Zhang's methods we used $\delta \in \{0.2, 0.5\}$, which are typical values for δ used in [4], [5]. First of all, the results show that we obtain an identical performance for the three objective functions. Hence, in terms of sensing performance, we are free to employ the optimization problem that leads to least computational complexity. Considering only the calculations for the three objective functions, we conclude that the sensing SINR and the MI are better choices than the CRLB, once the latter needs AoA information, which implies using some algorithm, such as multiple signal classification (MUSIC) [25] or estimation of signal parameters via rotational invariance (ESPRIT) [26], that increases computational complexity. For the former two, we only need sensing channel estimation, which can be performed transmitting pilot symbols in an upload link. This result also shows is that the proposed methods improve P_d when compared to M1-Zhang and M2-Zhang for all RCS variance values, while keeping the communication performance at a minimum desired level.

The last result, shown in Fig. 5, is the radiation pattern for the transmitter antenna. We also compare the beam pattern obtained with the multibeam method presented in this paper with the ones obtained with M1-Zhang and M2-Zhang. As we can see, our method achieves higher power at the desired directions, at the expense of presenting higher sidelobes between both of them. On the other hand, as the angle grows further from the UE and the targets directions, the sidelobes become smaller for our method, which demonstrates that it tends to concentrate the power in the specified directions.

V. Conclusion

In this work, we developed three strategies to optimize the power allocation between communication and sensing in a bi-static JCAS system, each one based on a different metric for the sensing: SINR, CRLB of the AoA estimator and the MI between the sensing channel and the echo signals at the receiver. We used an appropriate multibeam scheme for the precoder vector that included a scalar coefficient controlling the power balance.

The numerical results show that the three strategies converge to same optimum value for the power coefficient. They also show the trade-off between communication and sensing when using the optimum value of the power coefficient and some static values: the optimum value for δ maintains a desired communication performance in the expense of the sensing at higher noise levels, while with static δ is the opposite.

Finally, we compared the radiation pattern obtained with the proposed multibeam scheme with the ones presented in [4]. We concluded that our method tends to produce a more efficient power distribution between the directions, concentrating it the communication and sensing beams, and reducing it otherwise.

For future works, we intend to analyse other metrics for sensing, as, for example, the capacity-distortion function developed in [27], and compare it with the ones presented in this paper. We also intend to upgrade the system model's complexity including an orthogonal frequency division multiplexing (OFDM) model for the transmitted signal and also considering moving targets.

Appendix A
Proof for CRLB

Our demonstration follows the one in [28]. First of all, we rewrite (4) as

$$\mathbf{y}[n] = \mathbf{A}_M(\Theta)\mathbf{s}[n] + \mathbf{n}[n],$$

where

$$\mathbf{s}[n] = \mathbf{\Gamma}\mathbf{A}_L^H(\Phi)\mathbf{w}[n]p[n]$$

is the signal arriving at the receiver antenna array. We define

$$\mathcal{Y} = \{\mathbf{y}[0], \cdots, \mathbf{y}[\lfloor \alpha N \rfloor - 1]\},$$

the set of all received signal samples in a frame. Considering we know $\mathbf{s}[n]$ at the receiver, we can write the maximum likelihood (ML) probability density function as

$$\begin{aligned} p(\mathcal{Y}|\Theta) &= \prod_{n=0}^{\lfloor \alpha N \rfloor -1} p(\mathbf{y}[n]|\Theta), \\ &= \prod_{n=0}^{\lfloor \alpha N \rfloor -1} C \cdot \exp\left\{-\frac{1}{\sigma_s^2}\|\mathbf{y}[n] - \mathbf{A}_M\mathbf{s}[n]\|^2\right\}, \\ &= C^{\lfloor \alpha N \rfloor} \cdot \exp\left\{-\frac{1}{\sigma_s^2}\sum_{n=0}^{\lfloor \alpha N \rfloor -1}\|\mathbf{y}[n] - \mathbf{A}_M\mathbf{s}[n]\|^2\right\}, \end{aligned}$$

where

$$C = \pi^{-M}\det(\sigma_s^2\mathbf{I}_M).$$

The log-likelihood function is

$$\log p(\mathcal{Y}|\Theta) = \lfloor \alpha N \rfloor \log C - \frac{1}{\sigma_s^2}\sum_{n=0}^{\lfloor \alpha N \rfloor -1}\|\mathbf{y}[n] - \mathbf{A}_M\mathbf{s}[n]\|^2.$$

Developing the right hand side of the previous equation and taking the derivative in relation to θ_i, we have

$$\frac{\partial}{\partial\theta_i}\log p(\mathcal{Y}|\Theta) = \frac{2}{\sigma_s^2}\sum_{n=0}^{\lfloor \alpha N \rfloor -1}\mathrm{Re}\left\{\frac{\partial}{\partial\theta_i}\left[\mathbf{s}^H[n]\mathbf{A}_M^H(\Theta)\mathbf{y}[n] - \frac{1}{2}\|\mathbf{A}_M(\Theta)\mathbf{s}[n]\|^2\right]\right\},$$

whose derivatives of the individual terms are

$$\begin{aligned} &\frac{\partial}{\partial\theta_i}\mathbf{s}^H[n]\mathbf{A}_M^H(\Theta)\mathbf{y}[n] = s_i^*[n]\left(\frac{\partial\mathbf{a}_M(\psi)}{\partial\psi}\right)_{\psi=\theta_i}^H\mathbf{y}[n], \\ &\frac{\partial}{\partial\theta_i}\|\mathbf{A}_M(\Theta)\mathbf{s}[n]\|^2 = \\ &= 2\mathrm{Re}\left\{s_i^*[n]\left(\frac{\partial\mathbf{a}_M(\psi)}{\partial\psi}\right)_{\psi=\theta_i}^H\mathbf{A}_M(\Theta)\mathbf{s}[n]\right\}, \end{aligned}$$

and $s_i[n]$ is the i-th element of $\mathbf{s}[n]$. Replacing these results in the derivative of the log-likelihood, we have

$$\frac{\partial}{\partial\theta_i}\log p(\mathcal{Y}|\Theta) = \frac{2}{\sigma_s^2}\sum_{n=0}^{\lfloor \alpha N \rfloor -1}\mathrm{Re}\left\{s_i^*[n]\left(\frac{\partial\mathbf{a}_M(\psi)}{\partial\psi}\right)_{\psi=\theta_i}^H\mathbf{n}[n]\right\},$$

for $i = 1, \cdots, K$. The collection of all the K derivatives in a vector is the gradient of the log-likelihood, which can be compactly written as

$$\nabla_\Theta \log p(\mathcal{Y}|\Theta) = \frac{2}{\sigma_s^2}\sum_{n=0}^{\lfloor \alpha N \rfloor -1}\mathrm{Re}\left\{\mathbf{S}^H[n]\mathbf{D}^H(\Theta)\mathbf{n}[n]\right\}.$$

The Fisher information matrix is defined as

$$\mathbf{F} = \mathbb{E}\left\{\nabla_\Theta \log p(\mathcal{Y}|\Theta) \cdot \nabla_\Theta^H \log p(\mathcal{Y}|\Theta)\right\},$$

which, replacing in the above expression the result for the gradient of the log-likelihood function, can be written as

$$\mathbf{F} = \frac{4}{\sigma_s^4}\sum_{n=0}^{\lfloor \alpha N \rfloor -1}\sum_{n=0}^{\lfloor \alpha N \rfloor -1}\mathbb{E}\left\{\mathrm{Re}(\mathbf{z}[n])\mathrm{Re}(\mathbf{z}^H[n])\right\},$$

where

$$\mathbf{z}[n] = \mathbf{S}^H[n]\mathbf{D}^H(\Theta)\mathbf{n}[n].$$

The above expectation can be developed as

$$\begin{aligned}\mathbb{E}\left\{\mathrm{Re}(\mathbf{z}[n])\mathrm{Re}(\mathbf{z}^H[n])\right\} &= \mathbb{E}\left\{\frac{\mathbf{z}[n]+\mathbf{z}^*[n]}{2}\cdot\frac{\mathbf{z}^H[n]+\mathbf{z}^T[n]}{2}\right\},\\ &= \frac{1}{2}\mathbb{E}\left\{\mathbf{z}[n]\mathbf{z}^H[n]\right\},\\ &= \frac{\sigma_s^2}{2}\mathbf{S}^H[n]\mathbf{D}^H(\Theta)\mathbf{D}(\Theta)\mathbf{S}[n],\end{aligned}$$

where we have implicitly assumed, as in [28], that $\mathbb{E}\{\mathbf{z}[n]\mathbf{z}^T[n]\} = 0$. Finally, we obtain

$$\mathbf{CRLB}(\Theta) = \left\{\frac{2}{\sigma_s^2}\sum_{n=0}^{\lfloor \alpha N\rfloor -1}\mathbf{S}^H[n]\mathbf{D}^H(\Theta)\mathbf{D}(\Theta)\mathbf{S}[n]\right\}^{-1}.$$

REFERENCES

[1] F. Liu, Y. Cui, C. Masouros, J. Xu, T. X. Han, Y. C. Eldar, and S. Buzzi, “Integrated sensing and communications: Toward dual-functional wireless networks for 6g and beyond,” *IEEE journal on selected areas in communications*, vol. 40, no. 6, pp. 1728–1767, 2022.

[2] J. A. Zhang, M. L. Rahman, K. Wu, X. Huang, Y. J. Guo, S. Chen, and J. Yuan, “Enabling joint communication and radar sensing in mobile networks—a survey,” *IEEE Communications Surveys & Tutorials*, vol. 24, no. 1, pp. 306–345, 2021.

[3] B. D. Van Veen and K. M. Buckley, “Beamforming: A versatile approach to spatial filtering,” *IEEE assp magazine*, vol. 5, no. 2, pp. 4–24, 1988.

[4] J. A. Zhang, X. Huang, Y. J. Guo, J. Yuan, and R. W. Heath, “Multibeam for joint communication and radar sensing using steerable analog antenna arrays,” *IEEE Transactions on Vehicular Technology*, vol. 68, no. 1, pp. 671–685, 2018.

[5] M. U. Baig, J. Vinogradova, G. Fodor, and C. Mollen, “Joint communication and sensing beamforming for passive object localization,” in *WSA & SCC 2023; 26th International ITG Workshop on Smart Antennas and 13th Conference on Systems, Communications, and Coding*. VDE, 2023, pp. 1–6.

[6] F. Liu, C. Masouros, A. P. Petropulu, H. Griffiths, and L. Hanzo, “Joint radar and communication design: Applications, state-of-the-art, and the road ahead,” *IEEE Transactions on Communications*, vol. 68, no. 6, pp. 3834–3862, 2020.

[7] Z. Shi and Z. Feng, “A new array pattern synthesis algorithm using the two-step least-squares method,” *IEEE signal processing letters*, vol. 12, no. 3, pp. 250–253, 2005.

[8] Y. Luo, J. A. Zhang, W. Ni, J. Pan, and X. Huang, “Constrained multibeam optimization for joint communication and radio sensing,” in *2019 IEEE Global Communications Conference (GLOBECOM)*. IEEE, 2019, pp. 1–6.

[9] Y. Luo, J. A. Zhang, X. Huang, W. Ni, and J. Pan, “Multibeam optimization for joint communication and radio sensing using analog antenna arrays,” *IEEE Transactions on Vehicular Technology*, vol. 69, no. 10, pp. 11 000–11 013, 2020.

[10] N. Zhao, Y. Wang, Z. Zhang, Q. Chang, and Y. Shen, “Joint transmit and receive beamforming design for integrated sensing and communication,” *IEEE Communications Letters*, vol. 26, no. 3, pp. 662–666, 2022.

[11] C. B. Barneto, S. D. Liyanaarachchi, T. Riihonen, L. Anttila, and M. Valkama, “Multibeam design for joint communication and sensing in 5g new radio networks,” in *ICC 2020-2020 IEEE International Conference on Communications (ICC)*. IEEE, 2020, pp. 1–6.

[12] C. B. Barneto, S. D. Liyanaarachchi, T. Riihonen, M. Heino, L. Anttila, and M. Valkama, “Beamforming and waveform optimization for ofdm-based joint communications and sensing at mm-waves,” in *2020 54th Asilomar Conference on Signals, Systems, and Computers*. IEEE, 2020, pp. 895–899.

[13] D. Xu, C. Liu, S. Song, and D. W. K. Ng, “Integrated sensing and communication in coordinated cellular networks,” *arXiv preprint arXiv:2305.01213*, 2023.

[14] F. Dong, F. Liu, and C. Masouros, “Phy tradeoff and resource allocation for isac,” in *Integrated Sensing and Communications*. Springer, 2023, pp. 151–177.

[15] Z. Behdad, Ö. T. Demir, K. W. Sung, E. Björnson, and C. Cavdar, “Power allocation for joint communication and sensing in cell-free massive MIMO,” in *GLOBECOM 2022-2022 IEEE Global Communications Conference*. IEEE, 2022, pp. 4081–4086.

[16] Z. Ni, J. A. Zhang, K. Yang, X. Huang, and T. A. Tsiftsis, “Multi-metric waveform optimization for multiple-input single-output joint communication and radar sensing,” *IEEE Transactions on Communications*, vol. 70, no. 2, pp. 1276–1289, 2021.

[17] M. D. Larsen, A. L. Swindlehurst, and T. Svantesson, “Performance bounds for MIMO-OFDM channel estimation,” *IEEE Transactions on Signal Processing*, vol. 57, no. 5, pp. 1901–1916, 2009.

[18] L. Xu, J. Li, P. Stoica, K. W. Forsythe, and D. W. Bliss, “Waveform optimization for MIMO radar: A cramer-rao bound based study,” in *2007 IEEE International Conference on Acoustics, Speech and Signal Processing-ICASSP'07*, vol. 2. IEEE, 2007, pp. II–917.

[19] R. Xu, L. Peng, W. Zhao, and Z. Mi, “Radar mutual information and communication channel capacity of integrated radar-communication system using MIMO,” *ICT Express*, vol. 1, no. 3, pp. 102–105, 2015.

[20] A. Liu, M. Li, M. Kobayashi, and G. Caire, “Fundamental limits for isac: Information and communication theoretic perspective,” in *Integrated Sensing and Communications*. Springer, 2023, pp. 23–52.

[21] M. Ahmadipour, M. Kobayashi, M. Wigger, and G. Caire, “An information-theoretic approach to joint sensing and communication,” *IEEE Transactions on Information Theory*, 2022.

[22] Ö. T. Demir, E. Björnson, L. Sanguinetti *et al.*, “Foundations of user-centric cell-free massive MIMO,” *Foundations and Trends® in Signal Processing*, vol. 14, no. 3-4, pp. 162–472, 2021.

[23] S. M. Kay, “Statistical signal processing: estimation theory,” *Prentice Hall*, vol. 1, 1993.

[24] J. Li and R. Compton, “Maximum likelihood angle estimation for signals with known waveforms,” *IEEE Transactions on Signal Processing*, vol. 41, no. 9, pp. 2850–2862, 1993.

[25] A. M. Elbir, “Deepmusic: Multiple signal classification via deep learning,” *IEEE Sensors Letters*, vol. 4, no. 4, pp. 1–4, 2020.

[26] W. Li, W. Liao, and A. Fannjiang, “Super-resolution limit of the esprit algorithm,” *IEEE transactions on information theory*, vol. 66, no. 7, pp. 4593–4608, 2020.

[27] A. Liu, Z. Huang, M. Li, Y. Wan, W. Li, T. X. Han, C. Liu, R. Du, D. K. P. Tan, J. Lu *et al.*, “A survey on fundamental limits of integrated sensing and communication,” *IEEE Communications Surveys & Tutorials*, vol. 24, no. 2, pp. 994–1034, 2022.

[28] P. Stoica and A. Nehorai, “Music, maximum likelihood, and cramer-rao bound,” *IEEE Transactions on Acoustics, speech, and signal processing*, vol. 37, no. 5, pp. 720–741, 1989.